Published in IET Control Theory and Applications
Received on 23rd March 2009
Revised on 17th August 2009
doi: 10.1049/iet-cta.2009.0144


ISSN 1751-8644

# Discrete-time neuroadaptive control using dynamic state feedback with application to vehicle motion control for intelligent vehicle highway systems

*W.U.N. Fernando*[1] *S. Kumarawadu*[2]

[1]*School of Electrical and Electronic Engineering, University of Manchester, Sackville Street Building, Sackville Street, Manchester M60 1QD, UK*
[2]*Department of Electrical Engineering, University of Moratuwa, Moratuwa 10400, Sri Lanka*
*E-mail: w.fernando@postgrad.manchester.ac.uk*

**Abstract:** Discrete time neuro-compensated dynamic state feedback control system for lateral and longitudinal control of intelligent vehicle highway systems (IVHS) is developed. A discrete time counterpart of the continuous time non-linear IHVS model is obtained in state-space form and the controller is analysed in three stages, with and without compensation mechanisms resulting in an implementation from low to high complexity. Gain parameters of the dynamic state feedback control are optimised with respect to a minimisation of a linear quadratic cost function. The weight convergence of the neuro-compensation algorithm is established in discrete time Lyapunov sense via a graphical method. The performance enhancement of each design stage of the controller is presented and compared with the aid of computer simulations.

## 1 Introduction

Automatic control of steering and speed of vehicles for intelligent vehicle highway systems (IVHS) have been researched extensively and still remain to be fully developed. Much research on IVHS has been focused on the continuous time domain [1–7]. However, microprocessor-based implementation of control algorithms and the realisation of embedded systems pose certain challenges to control engineers. These may be associated with performance, feasibility and/or considerations on long-term economic viability of such designs. Highway vehicles are fast moving systems with the states changing so rapidly. Hence, taking into account the effects of finite sampling is particularly important in controller design. Furthermore, certain characteristics observed in the theoretical or simulated continuous time controllers maybe limited in a discrete time implementation with restricted microprocessor performance, computational throughput, signal processing delays, actuation delays and switching delays [7, 8]. Therefore rigorous analysis of the discrete time control is essential to guarantee certain general performance criteria prior to fabrication and implementation of automatic control systems for vehicles.

Much of the research done in neuro-adaptive control is in continuous time domain [9, 10] with proven neural network (NN) performance and guaranteed weight convergence in Lyapunov sense. The importance of discrete time analysis has been identified in [11, 12] and analysed for a class of non-linear dynamic systems. IVHS belongs to a class of non-linear discrete time systems that inherently have fast state changes between two sampling instances. Adaptive control and the approach for guarantee of stability in discrete time domain is not straightforward. The control system design presented in this paper addresses issues such as discrete time-domain stability and weight convergence. The proof of weight and error convergence presented in



© The Institution of Engineering and Technology 2010

Section 4 is based on discrete time Lyapunov theory. A formative theoretical approach is developed with a conservative stability criterion. The proof is verified with further graphical illustrations.

Different NN-based techniques have been developed in the past for the control of non-linear systems. A widely researched class of neuro-adaptive controllers is based on system identification [13, 14], where a proper model is selected for controller design and NN are used for the adjusting of its parameters for error convergence. The control parameters are thus adjusted accordingly. In contrast [15, 16], attempts to establish the inverse dynamics with NNs and provide control with error convergence. A different class of techniques that have been overlooked is the adaptive control of Lipschitz non-linear discrete time systems [17], with neuro-adaptive feed-forward for unmodelled dynamics compensation. The method of IVHS control presented in this paper deals with a case of Lipschitz non-linear discrete time systems, and control with the classical dynamic state feedback with non-linear coupling compensation and NN-based unmodelled dynamics compensation, which has not been dealt in literature in the past.

This work is motivated by the controller design by Kumarawadu and Lee [9] in continuous time domain. In this paper in contrast, the analysis and design are completely in the discrete time domain making it much closer to direct industrial microprocessor-based implementation. The natural benefit of using whatever reliable model information that is available in this controller is preserved by the dynamic state feedback together with the strong learning capabilities of the NNs. Furthermore, this work also lays the foundation for future analysis of sensor fusion studies in discrete time domain and controller performance with multifarious sensors such as machine vision or GPS together with the radar and magnetic marker-based systems.

Position/speed sensing in IVHS may be done with respect to either an earth-fixed reference frame or body reference frame or both. Typical fixed on earth reference frame-based systems utilise GPS measurements or roadbed placed magnetic markers [18]. In contrast, body reference frame-based systems rely on measurements from radar or machine vision [1, 6]. This is largely seen in platooning operations of IVHS where the vehicle is intended to follow the preceding vehicle keeping a predefined spacing. The IVHS considered in this work is based on the combination of fixed reference frame system for lateral control and a body reference frame system for longitudinal control of platooning operation. The lateral controller regulates lateral displacement by the measurement of magnetic marker position whereas the longitudinal controller regulates the vehicle speed and maintains the spacing between vehicles using radar measurements. The lateral dynamics and the longitudinal dynamics are coupled, and can be divided as kinetic coupling, tire force coupling and weight coupling [6]. The coupled nature between the two channels maybe addressed by merging both systems into one [8, 19] or considering two separate control problems [2, 20] combined with coupling compensation mechanisms. The former is adopted in this paper hence taking into account the inherent coupling effects that are dominant at higher speeds, accelerations and when the steering angle is large at lower road curvatures.

Automated vehicle control techniques seen in literature are linear control techniques [11], dynamic decoupling techniques [7], robust control techniques such as sliding mode control and $H_\infty$ control [2, 21–23] and intelligent methods such as fuzzy inference systems [1, 3, 4] or direct adaptive NN-based control [5, 20]. Economic factors bring forth the requisite of evaluation of multiple technologies before commissioning. The debatable trade-off of performance over cost has to be established. The complexity of the controller has to be justified with the improvement of performance. Accordingly, this paper presents the performance of the controller in three versions, viz., (a) system with neglected coupling terms and unmodelled dynamics, control law defined as a linear dynamic state feedback tracking problem; (b) system with neglected unmodelled dynamics, control law defined as a linear dynamic state feedback tracking problem with coupling compensation; (c) control law defined as a linear dynamic state feedback tracking problem, with coupling compensation and neuro-compensation of unmodelled dynamics. The complexity of the controller is highest with the neuro-compensation (c) and the simplest form (a), which is implementable with a low-end microprocessor. Coupling terms and unmodelled dynamics are neglected at the expense of tracking accuracy, yet may provide with satisfactory performance [6].

The complex three-degree-of-freedom (3-DOF) continuous time dynamic model of the Sevrin (Mitsubishi Motors, Taiwan, ROC) passenger wagon [9] is extended to the discrete time domain with approximations that significantly simplify the control law formulation and implementation. The control law is based on this discrete time version of the vehicle dynamic model instead of direct discretisation of the continuous time control law. This gives way to analysis of the dynamics in discrete time state-space canonical form. Closed-loop stability of the dynamic state feedback control is established and the feedback gains are optimised considering the system as a discrete time linear quadratic tracking problem. This resembles the PID control law formulation in the continuous domain.

Section 2 presents the non-linear 3-DOF discrete time dynamic model of the vehicle. The dynamic state feedback control law and the coupling compensation are derived from this model. Section 3 illustrates the formulation of the three versions of the controller, and establishes the


© The Institution of Engineering and Technology 2010

doi: 10.1049/iet-cta.2009.0144

closed-loop stability with suitable assumptions. Section 4 presents the formulation of the neuro-compensation of unmodelled dynamics and establishes the weight and error convergence in discrete time Lyapunov sense using a graphical technique. Simulation test results are given in Section 5 to visualise the performance of the each controller version under severe acceleration and road curvature conditions. Section 6 concludes this paper.

## 2 Discrete-time description of vehicle dynamics

Extensive analysis has been done with the 'Sevrin' (Mitsubishi Motors, Taiwan, ROC) and a complex 3-DOF dynamic models have been developed in [9] (see Table 1). The vehicle model is a FWD/FWS system with 100/0 brake torque distribution, see Fig. 1.

**Table 1** Parameter values of the Sevrin vehicle system

| Symbol | Quantity | Value |
|---|---|---|
| $m$ | total mass of the vehicle | 1760 kg |
| $I_Z$ | yaw inertia | 3332 kg m$^2$ |
| $f$ | rolling friction coefficient | 0.02 |
| $a$ | distance-front wheel to CG | 1.193 m |
| $L$ | wheel-base ($a+b$) | 2.78 m |
| $d_S$ | distance from front bumper to CG | 2.103 m |
| $C_f$ | cornering stiffness – front | 131 391 N/rad |
| $C_r$ | cornering stiffness – rear | 115 669 N/rad |
| $k_L$ | aerodynamics lift parameter | 0.008 Ns$^2$/m$^2$ |
| $k_D$ | aerodynamics drag parameter | 0.49 Ns$^2$/m$^2$ |

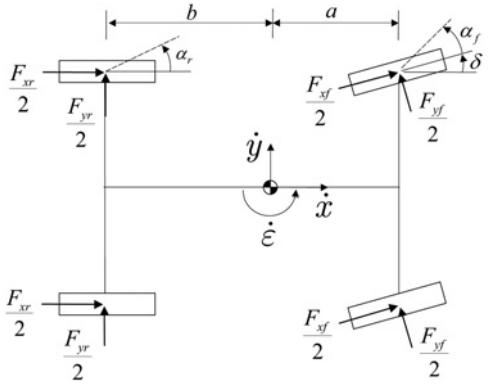


**Figure 1** *Vehicle model*

### 2.1 Continuous-time version of vehicle dynamics

Continuous time-domain equations of motion of the vehicular system in Fig. 1 are [9]

$$m\ddot{x} = F_{xr} + F_{xf}\cos\delta - F_{yf}\sin\delta + m\dot{\varepsilon}\dot{y} - k_D\dot{x}^2 \quad (1)$$

$$m\ddot{y} = F_{yr} + F_{xf}\sin\delta + F_{yf}\cos\delta - m\dot{\varepsilon}\dot{x} \quad (2)$$

$$I_z\ddot{\varepsilon} = aF_{xf}\sin\delta + aF_{yf}\cos\delta - bF_{yr} \quad (3)$$

where $x$, $y$ and $\varepsilon$ are the coordinates in the vehicle body reference frame and the yaw angle. $F_{xr}$, $F_{yr}$, $F_{xf}$, $F_{yf}$ are the tire forces with subscript r representing the rear wheel and f representing the front wheel. $\delta$ is the steering angle.

### 2.2 Discrete-time version of vehicle dynamics

Consider a system described by Newton's second law of motion with a non-linear specific force $f$ [24]

$$\ddot{x}(t) = f(\bullet) \quad (4)$$

where $f$ is a smooth, infinitely differentiable function of known real variables. At $t = t_k$ time instant, the Taylor expansion of $\dot{x}$ for a time step $T_s$ is given by

$$\dot{x}(t_k + T_s) = \dot{x}(t_k) + \sum_{j=1}^{\infty} \frac{T_s^j}{j!}\frac{\partial^j \dot{x}(t)}{\partial t^j}\bigg|_{t=T_s} \quad (5)$$

The Taylor expansion method provides a finite polynomial representation of the system and is used for the discretisation of the non-linear vehicle dynamics. Substitution of (4) into (5) and with neglected higher order terms, an approximate discrete model is be obtained. Considering the state-space form of (1), (2), (3) the state variables at $t = T_s$ are selected as

$$z_1(k) = \dot{x}(k)|_{t=kT_s} \quad (6)$$

$$z_2(k) = y(k)|_{t=(k-1)T_s} \quad (7)$$

$$z_3(k) = y(k)|_{t=kT_s} \quad (8)$$

$$z_4(k) = \dot{\varepsilon}(k)|_{t=kT_s} \quad (9)$$

The discrete-time index is denoted by $k(>0)$. The state-space



© The Institution of Engineering and Technology 2010

model can be constructed as

$$\begin{bmatrix} z_1(k+1) \\ z_2(k+1) \\ z_3(k+1) \\ z_4(k+1) \end{bmatrix} = \begin{bmatrix} 1 & 0 & 0 & 0 \\ 0 & 0 & 1 & 0 \\ 0 & -1 & 2 & 0 \\ 0 & 0 & 0 & 1 \end{bmatrix} \begin{bmatrix} z_1(k) \\ z_2(k) \\ z_3(k) \\ z_4(k) \end{bmatrix} + \frac{\partial}{\partial t} \begin{bmatrix} T_s \dot{x}(k) \\ 0 \\ T_s^2 \dot{y}(k) \\ T_s \dot{\varepsilon}(k) \end{bmatrix} \Bigg|_{t=T_s} + \begin{bmatrix} \vartheta_1(T_s) \\ \vartheta_2(T_s) \\ \vartheta_3(T_s) \\ \vartheta_4(T_s) \end{bmatrix} \quad (10)$$

where the vector of higher order terms at $t = kT_s$ is given by

$$\begin{bmatrix} \vartheta_1(T_s) \\ \vartheta_2(T_s) \\ \vartheta_3(T_s) \\ \vartheta_4(T_s) \end{bmatrix} = \begin{bmatrix} \sum_{j=2}^{\infty} \frac{T_s^j}{j!} \frac{\partial^j \dot{x}(t)}{\partial t^j} \\ 0 \\ \sum_{j=1}^{\infty} \frac{T_s^j}{j!} \frac{\partial^j \dot{y}(2t) - \dot{y}(t)}{\partial t^j} + \sum_{j=2}^{\infty} \frac{T_s^{j+1}}{j!} \frac{\partial^j \dot{y}(t)}{\partial t^j} \\ \sum_{j=2}^{\infty} \frac{T_s^j}{j!} \frac{\partial^j \dot{\varepsilon}(k)}{\partial t^j} \end{bmatrix}$$

The non-linear vector in (10) can be expanded at as

$$\frac{\partial}{\partial t} \begin{bmatrix} T_s \dot{x}(k) \\ 0 \\ T_s^2 \dot{y}(k) \\ T_s \dot{\varepsilon}(k) \end{bmatrix} \Bigg|_{t=T_s} = \begin{bmatrix} \{z_4(k)(z_3(k) - z_2(k)) \\ -k_D \frac{T_s}{m} z_1^2(k)\} \\ 0 \\ -T_s^2 z_4(k) z_1(k) \\ 0 \end{bmatrix} + \frac{T_s}{m} \begin{bmatrix} F_{xr}(k) + F_{xf}(k)\cos\delta(k) - F_{yf}(k)\sin\delta(k) \\ 0 \\ T_s\{F_{yr}(k) + F_{xf}(k)\sin\delta(k) + F_{yf}(k)\cos\delta(k)\} \\ \frac{m}{I_z}\{aF_{xf}(k)\sin\delta(k) \\ + aF_{yf}(k)\cos\delta(k) - bF_{yr}(k)\} \end{bmatrix} \quad (11)$$

Longitudinal forces $F_{xr}$ and $F_{xf}$ can be written as

$$F_{xf}(k) = F - f\left(\frac{b}{a+b}\right)(mg - k_L z_1^2(k)) \quad (12)$$

$$F_{xr}(k) = -f\left(\frac{a}{a+b}\right)(mg - k_L z_1^2(k)) \quad (13)$$

where $F = F_{\text{traction}} - F_{\text{braking}}$ is the net force exerted on the wheels.

With a linear tire model [9, 25], the lateral forces at $t = kT_s$ can be written as

$$F_{yr}(k) = -C_r \alpha_r(k) \quad (14)$$

$$F_{yf}(k) = -C_f \alpha_f(k) \quad (15)$$

where $\alpha_r(k)$, $\alpha_f(k)$ are the rear and front slip angles. Assuming equal slip angles on the right and left [9], it will be written in discrete form in terms of the model states as

$$\alpha_f(k) = \frac{z_3(k) - z_2(k) + T_s a z_4(k)}{T_s z_1(k)} - \delta(k) \quad (16)$$

$$\alpha_r(k) = \frac{z_3(k) - z_2(k) - T_s b z_4(k)}{T_s z_1(k)} \quad (17)$$

Using a small angle approximation, $\cos\delta \simeq 1$, $\sin\delta \simeq \delta$ and substituting (12)–(17) into (11) yields a system with a non-linear vector which can be rewritten in terms of a controllable non-linear vector $g[u(k)]$ and a compensable vector $h[u(k)]$, where the control input $u(k) = [F(k), \delta(k)]^T$

$$\frac{\partial}{\partial t} \begin{bmatrix} T_s \dot{x}(k) \\ 0 \\ T_s^2 \dot{y}(k) \\ T_s \dot{\varepsilon}(k) \end{bmatrix} \Bigg|_{t=T_s} = g[u(k)] + h[z(k)] \quad (18)$$

where

$$g[u(k)] = \frac{T_s}{m} \begin{bmatrix} F - F_{yf}(k)\delta(k) \\ 0 \\ T_s(F_{xf}(k)\delta(k) + C_f\delta(k)) \\ \frac{ma}{I_z}(F_{xf}(k)\delta(k) + C_f\delta(k)) \end{bmatrix}$$

$$h[z(k)] = \begin{bmatrix} \left\{-f\frac{T_s}{m}(mg - k_L z_1^2(k)) \right. \\ \left. + z_4(k)(z_3(k) - z_2(k)) - k_D \frac{T_s}{m} z_1^2(k)\right\} \\ 0 \\ -T_s\left\{C_r\left(\frac{z_3(k) - z_2(k) - T_s b z_4(k)}{m z_1(k)}\right)\right. \\ \left. + C_f\left(\frac{z_3(k) - z_2(k) + T_s a z_4(k)}{m z_1(k)}\right) + T_s z_4(k) z_1(k)\right\} \\ \frac{1}{I_z}\left\{-aC_f\left(\frac{z_3(k) - z_2(k) + aT_s z_4(k)}{z_1(k)}\right)\right. \\ \left. + bC_r\left(\frac{z_3(k) - z_2(k) - bT_s z_4(k)}{z_1(k)}\right)\right\} \end{bmatrix}$$

Let $z(k) = [z_1(k)\ z_2(k)\ z_3(k)\ z_4(k)]^T$ and $\vartheta(T_s) = [\vartheta_1(T_s)\ 0\ \vartheta_3(T_s)\ \vartheta_4(T_s)]^T$ be the state vector and the higher order term of discretisation. Then the complete approximate system can be rewritten as

$$z(k+1) = Az(k) + Bg[u(k)] + h[z(k)] + \vartheta(T_s) \quad (19)$$

where

$$A = \begin{bmatrix} 1 & 0 & 0 & 0 \\ 0 & 0 & 1 & 0 \\ 0 & -1 & 2 & 0 \\ 0 & 0 & 0 & 1 \end{bmatrix}, \quad B = 1/m \begin{bmatrix} 1 & 0 & 0 & 0 \\ 0 & 1 & 0 & 0 \\ 0 & 0 & 1 & 0 \\ 0 & 0 & 0 & 1 \end{bmatrix}$$

The input vector for the lateral dynamics and yaw dynamics


© The Institution of Engineering and Technology 2010

doi: 10.1049/iet-cta.2009.0144

are mutual, the system can be solved in terms of combined lateral/yaw control input and a longitudinal control.

$$g[u(k)] = \left[ g_x \;\; 0 \;\; g_{y\varepsilon} \;\; \left(\frac{ma}{T_s I_z}\right) g_{y\varepsilon} \right]^{\mathrm{T}}$$

## 3 Control algorithm

The discrete-time control algorithm is given here. Fig. 2 shows the overview of the controller structure. The three versions of the controller are (i) without coupling and neuro compensation, (ii) with only coupling compensation, and (iii) the full system with coupling and neuro compensation. Different performance improvements with each version of control law are identified. The basis of the control law is to simultaneously regulate longitudinal speed error $e_1(k)$ and the lateral spacing error $e_3(k)$ such that the vehicle tracks the speed of the preceding vehicle, while maintaining the spacing in between and the lateral deviation from the road centreline at a desired level.

$$e_1(k) = z_1^*(k) - z_1(k) \tag{20}$$

$$e_3(k) = z_3^*(k) - z_3(k) \tag{21}$$

IVHS belongs to a class of non-linear discrete time systems that inherently have fast state changes between two sampling instances. Continuous-time control design alone cannot guarantee the required stability of such systems as the continuity of signals is in a much disturbed state. So far very little research has been done in the area of adaptive control of such systems and the assessment of stability in discrete time domain. The controller presented here addresses issues such as discrete time-domain stability and weight convergence.

The superiority of the proposed control structure appear from the operational requirements of IVHS, such as controller fault tolerance, safety, low computational intensity, ease of implementation in addition to overall stability, robustness and fast error convergence. The controller presented herein is preferred for the application in IVHS over neuro-adaptive controllers based on system parameter optimisation schemes due to its partial redundancy. This system is likely to operate with satisfactory performance even if the operation of NN module is hindered because of any unanticipated operating condition. Neuro-adaptive controllers based on parameter optimisation are concentrated on plant parameters and controller gains. Thus any undesired modification of the vehicle dynamics will not be adequately compensable via the controller. In contrast, the proposed controller has a higher degree of fault tolerance due to NNs not being priory dependent upon a plant model. Any plant variation will be compensated by the NN. The controller method is developed such that the NNs are implemented in modular fashion, and provides ease of implementation. The use of radial basis function (RBF) NNs reduces the computational intensity of the NNs and is further reduced because of the single output modular implementation of the NNs. The NN output maybe used for sensor fault identification and isolation.

### 3.1 Control law as a linear dynamic state feedback tracking problem with neglected coupling terms and unmodelled dynamics

We stack the coupled terms $h[z(k)]$, discretisation error $\vartheta(T_s)$, parameter estimation discrepancies and unmodelled dynamics together to form a single term, $\xi$

$$\xi = [\,\xi_1 \quad 0 \quad \xi_3 \quad \xi_4\,]$$
$$|\xi_1| < \xi_{1N}, \quad |\xi_3| < \xi_{3N}, \quad |\xi_4| < \xi_{4N}$$

where $\xi_{1N}$, $\xi_{3N}$, $\xi_{4N} \in \Re$ are practical bounds of the neglected terms in the longitudinal and lateral systems. The control laws based on dynamic state feedback are

$$g_x = \frac{\hat{m}}{T_s}\{-k_{Px}e_1(k) - k_{Ix}(\theta_{Ix}(k) - \Delta_x)\} \tag{22}$$

$$g_y = \frac{\hat{m}}{T_s^2}\{-k_{Py,1}e_3(k) - k_{Py,2}e_2(k) - k_{Iy}\theta_{Iy}(k)\} \tag{23}$$

where $\Delta_x$ is the desired longitudinal spacing input. $\theta_{Ix}(k)$ and $\theta_{Iy}(k)$ are the integrated control error terms computed as

$$\theta_{Ix}(k+1) = a_{Ix}\theta_{Ix}(k) + b_{Ix}[z_1^*(k) - z_1(k)] \tag{24}$$

$$\theta_{Iy}(k+1) = a_{Iy}\theta_{Iy}(k) + b_{Iy}[z_2^*(k) - z_2(k)] \tag{25}$$

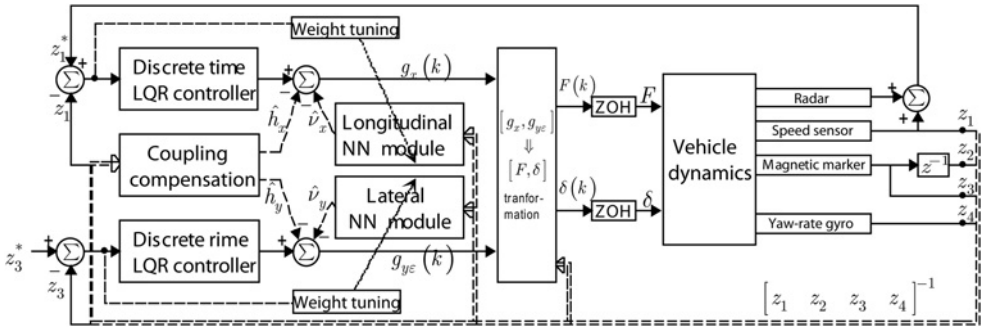


**Figure 2** *IVHS control system overview*



© The Institution of Engineering and Technology 2010

Let $a_{Ix} = a_{Iy} = 1$ and $b_{Ix} = b_{Iy} = T_s$. Control laws (22) and (23) allow us to write (19) longitudinal error dynamics as

$$e_1(k+1) - (k_{Px}+1)e_1(k) - k_{Ix}(\theta_{Ix}(k) - \Delta_x) + \xi_1 = 0 \quad (26)$$

where $e_1(k) = z_1^*(k) - z_1(k)$, $z_1^*(k)$ is the speed of the preceding vehicle. Equation (22) results $|e_1(k)| \to 0$ as $k \to \infty$ for every initial error condition $e_1(k_0)$ assuming a slow varying $\xi_1$. In other words the error is asymptotically brought to zero while keeping the longitudinal spacing (integrated control error term) at the desired level

$$\theta_{Ix}(k) = \Delta_x - \xi_1/k_{Ix} \quad (27)$$

where $\Delta_x$ is determined such that $\Delta_x > \xi_{1N}/k_{Ix}$ under all extreme conditions.

Lateral error dynamics can be written as

$$e_3(k+1) - (k_{Py,1}+2)e_3(k) - (k_{Py,2}-1)e_2(k) - k_{Iy}\theta_{Iy}(k) + \xi_3 = 0 \quad (28)$$

where $e_3(k) = z_3^*(k) - z_3(k)$, $z_3^*(k)$ is the desired lateral spacing from the road centre line. Control law (23) results $|e_3(k)| \to 0$ as $k \to \infty$ for every initial error condition $e_3(k_0)$ assuming a slow varying $\xi_3$. That is, the error is asymptotically brought to zero.

*3.1.1 Determination of controller gains:* Both the longitudinal and the lateral dynamics are written as

$$\gamma_x(k+1) = A_x\gamma_x(k) + B_x\xi_1 \quad (29)$$

and

$$\gamma_y(k+1) = A_y\gamma_y(k) + B_y\xi_3 \quad (30)$$

where

$$\gamma_x(k) = \begin{bmatrix} e_1(k) \\ \phi_{Ix}(k) \end{bmatrix}, \quad \gamma_y(k) = \begin{bmatrix} e_2(k) \\ e_3(k) \\ \theta_{Iy}(k) \end{bmatrix}$$

and $\phi_{Ix}(k) = \theta_{Ix}(k) - \Delta_x$

$$A_x = \begin{bmatrix} (k_{Px}+1) & k_{Ix} \\ b_{Ix} & a_{Ix} \end{bmatrix}, \quad B_x = \begin{bmatrix} -1 \\ 0 \end{bmatrix}$$

$$A_y = \begin{bmatrix} 0 & 1 & 0 \\ (k_{Py,2}-1) & (k_{Py,1}+2) & k_{Iy} \\ 0 & b_{Iy} & a_{Iy} \end{bmatrix}, \quad B_y = \begin{bmatrix} 0 \\ -1 \\ 0 \end{bmatrix}$$

The gains are obtained by discrete linear quadratic optimisation. This technique is widely used in literature [26], and is known to provide superior system gain and phase margins [27]. The emphasis is on the minimisation of a quadratic cost function of the form

$$J = \sum \gamma^{\mathrm{T}}(k)Q\gamma(k) + \xi^{\mathrm{T}}(k)R\xi(k) \quad (31)$$

where $\gamma(k)$ is the state vector and $\xi(k)$ is the input vector of the dynamic state feedback system (26) or (27). The matrices $Q$ and $R$ are the state cost matrix $Q = Q^{\mathrm{T}} \succeq 0$ and input cost matrix $R = R^{\mathrm{T}} \succeq 0$, respectively. Notation $\succeq 0$ represents positive definiteness. The gain values are obtained as

$$k_{Px} = -0.6337, \quad k_{Ix} = -1.9391$$
$$k_{Py,1} = -0.5260, \quad k_{Py,2} = 0.4163, \quad k_{Ix} = -0.0764$$

## 3.2 Control law as a linear dynamic state feedback tracking problem with coupling compensation and neglected unmodelled dynamics

The control scheme, (22) and (23), is augmented with a coupling compensation term calculated in terms of measured state variables. Then, the control law becomes

$$g_x = \frac{\hat{m}}{T_s}\{-k_{Px}e_1(k) - k_{Ix}(\theta_{Ix}(k) - x_d)\} - \widehat{h}_x \quad (32)$$

$$g_y = \frac{\hat{m}}{T_s^2}\{-k_{Py,1}e_3(k) - k_{Py,2}e_2(k) - k_{Iy}\theta_{Iy}(k)\} - \widehat{h}_y \quad (33)$$

where

$$\widehat{h}_x = \left\{-f\frac{T_s}{\hat{m}}(\hat{m}g - k_L z_1^2(k)) + z_4(k)(z_3(k) - z_2(k)) - k_{\mathrm{D}}\frac{T_s}{\hat{m}}z_1^2(k)\right\} \quad (34)$$

$$\widehat{h}_y = -T_s\left\{C_{\mathrm{r}}\left(\frac{z_3(k) - z_2(k) - T_s b z_4(k)}{\hat{m}z_1(k)}\right) + C_{\mathrm{f}}\left(\frac{z_3(k) - z_2(k) + T_s a z_4(k)}{\hat{m}z_1(k)}\right) + T_s z_4(k)z_1(k)\right\} \quad (35)$$

which yields longitudinal and lateral error dynamics of (19) as

$$e_1(k+1) - (k_{Px}+1)e_1(k) - k_{Ix}(\theta_{Ix}(k) - \Delta_x) + \xi_1' = 0 \quad (36)$$

$$e_3(k+1) - (k_{Py,1}+2)e_3(k) - (k_{Py,2}-1)e_2(k) - k_{Iy}\theta_{Iy}(k) + \xi_3' = 0 \quad (37)$$

where $\xi_1'$ and $\xi_3'$ represents the discretisation error $\vartheta(T_s)$, parameter estimation discrepancies and unmodelled dynamics. $|\xi_1'| < \xi_{1N}'$, $|\xi_3'| < \xi_{3N}'$. $\xi_{1N}'$ and $\xi_{3N}'$ are practical bounds of the neglected terms in the longitudinal and lateral systems with control laws (32), (33). Under ideal circumstances the estimated compensation terms effectively cancels the non-linear vector, resulting in $\xi_{1N}' < \xi_{1N}$, $\xi_{3N}' < \xi_{3N}$. Thus an improvement of the overall system performance can be


© The Institution of Engineering and Technology 2010

doi: 10.1049/iet-cta.2009.0144

anticipated with better tracking of lateral and longitudinal references. The closed-loop stability can be established in a similar manner to the case of 3.1. The computation of the compensation terms require multiplication and division subroutines which demand more computational resources in each microprocessor cycle.

### 3.3 Control law defined as a linear dynamic state feedback tracking problem, with coupling compensation and neuro-compensation of unmodelled dynamics and discretisation approximations

The control scheme described by (32) and (33) is further augmented with an adaptive neuro-compensation term. The inputs to the NN are in terms of the measured state variables. Then, the control law becomes

$$g_x = \frac{\hat{m}}{T_s}\{-k_{Px}e_1(k) - k_{Ix}(\theta_{Ix}(k) - x_d)\} - \widehat{b}_x - \widehat{\nu}_x \quad (38)$$

$$g_y = \frac{\hat{m}}{T_s^2}\{-k_{Py,1}e_3(k) - k_{Py,2}e_2(k) - k_{Iy}\theta_{Iy}(k)\} - \widehat{b}_y - \widehat{\nu}_y \quad (39)$$

where $\widehat{\nu}_x$ and $\widehat{\nu}_y$ are the NN output signals. The longitudinal and lateral error dynamics of (19) can be rewritten as

$$e_1(k+1) - (k_{Px}+1)e_1(k) - k_{Ix}(\theta_{Ix}(k) - \Delta_x) + \xi_1'' = 0 \quad (40)$$

$$e_3(k+1) - (k_{Py,1}+2)e_3(k) - (k_{Py,2}-1)e_2(k) - k_{Iy}\theta_{Iy}(k) + \xi_3'' = 0 \quad (41)$$

where $\xi_1'' = (\nu_x + \varepsilon_x) - \widehat{\nu}_x$ and $\xi_3'' = (\nu_y + \varepsilon_y) - \widehat{\nu}_y$.

$\nu_x$, $\nu_y$ correspond to the ideal weights and $\varepsilon_x$, $\varepsilon_x$ correspond to the NN approximation error terms with practical bounds given by $|\varepsilon_x| < \varepsilon_{xN}$ and $|\varepsilon_y| < \varepsilon_{yN}$. Under ideal circumstances the NN outputs cancel the other terms. This results $\xi_1'' \to 0$ , $\xi_3'' \to 0$ and the error in longitudinal and lateral dynamics being asymptotically brought to zero, while maintaining the longitudinal and lateral spacing at the desired spacing values.

This scheme requires a separate module with neural networking capability to be operated in parallel with the microprocessor for highest performance. As a consequence the implementation will require special purpose hardware for debugging, testing and verification of the embedded vehicle control system.

#### 3.3.1 Obtaining the real control inputs F and δ:

The following transformation converts the controller outputs $g_x$, $g_{y\varepsilon}$ to vehicle steering angle $\delta(k)$ and force $F$. With (12)–(17) we may write

$$g_x = F(k) + \hat{C}_f\beta_1(k)\delta(k) \quad (42)$$

$$g_{y\varepsilon} = (F(k) - \beta_2(k))\delta(k) + \hat{C}_f\delta(k) \quad (43)$$

where assuming $(\delta(k))^2 \simeq 0$ [9]

$$\beta_1(k) = \frac{z_3(k) - z_2(k) + T_s\hat{a}z_4(k)}{T_s z_1(k)} \quad (44)$$

$$\beta_2(k) = \hat{f}\frac{\hat{b}}{\hat{a}+\hat{b}}(mg - k_L z_1(k)) \quad (45)$$

Substitution of (42) into (43) yields a quadratic equation of the form

$$a_0(\delta(k))^2 + b_0\delta(k) + c_0 = 0 \quad (46)$$

where

$$a_0 = \hat{C}_f\beta_1(k)(\delta(k))^2 \quad (47)$$

$$b_0 = (g_x + \hat{C}_f - \beta_2(k)) \quad (48)$$

$$c_0 = g_{y\varepsilon} \quad (49)$$

This gives

$$\delta(k) = \begin{cases} \dfrac{-b_0 - \sqrt{b_0^2 - a_0c_0}}{2a_0} & \text{if } a_0 \neq 0 \\ -\dfrac{c_0}{b_0} & \text{if } a_0 = 0 \end{cases} \quad (50)$$

Net force $F(k)$ is obtained using (42) and (43).

## 4 Analysis of the neuro-compensation technique

NNs are universal approximators, that is, they are capable of replicating any well behaved non-linear function with adequate accuracy [28–30]. Two of the most widely researched classes of NN architectures utilised for function approximation are the multilayer perceptron (MLP) and the RBFNNs [31].

The MLPNNs are based on a structure where inputs are passed through non-linear functionality to produce an output. The MLPNN may have one or more hidden layers. The hidden layer node output is a function of the inner product of the input vector and the synaptic weight vector attached to the node. Activation functions that have been widely researched in the application of function approximation with MLPNNs are the sigmoid function, hyperbolic tangent function [32]. The reader is referred to [33], for a comprehensive overview.



© The Institution of Engineering and Technology 2010

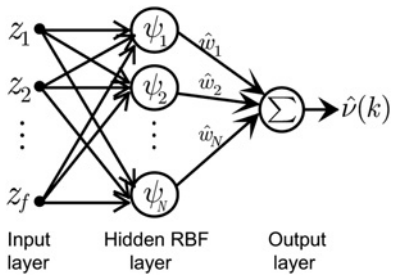


**Figure 3** *RBF NN architecture*

In contrast RBFNNs have only one hidden layer. The RBFNN architecture used in this research is shown in Fig. 3. The input vector is not weighted. Instead the hidden layer node output is defined as a function of the normalised euclidean distance between input vector and the centre of that unit. The orthogonal least squares algorithm [34] is typically used for the selection of the RBF unit centres. The most commonly used activation function with RBFNNs is the Gaussian [35] and is used in this research as well.

RBFNNs are popular because of its simplicity, fast learning [36] and universal approximation properties [37]. Furthermore, hardware implementation has shown that RBFNNs perform much faster, require less processing resources and storage [38] compared with MLPNN. Therefore in this work, RBFNNs are used and proof of guaranteed weight convergence is sought in the discrete time domain. NNs are implemented as two separate subnets: $x$-subnet and $y$-subnet which takes care of the longitudinal and the lateral compensations tasks separately. Hence, the weight adaptation law parameters can be independently chosen and weights be separately initialised to obtain a faster weight adaptation.

## 4.1 Radial basis function

The activation function (RBF) NNs that is adopted in this work is of the form

$$\psi_i(z(k)) = \exp\left[-\sum_{j=1}^{f}\left(\frac{z_j(k)-c_{ij}}{\sqrt{2}\sigma_{ij}}\right)^2\right]; \quad i = 1, 2, \ldots, n \tag{51}$$

$\mathbf{z} = \begin{bmatrix} z_1(k) & z_2(k) \cdots z_f(k) \end{bmatrix}^{\mathrm{T}}$ is the input vector. $c_{ij}$ and $\sigma_{ij}$ are the centre state and the standard deviations of the Gaussians associated with each element of input vector, respectively. $n$ is the number of hidden-layer neurons.

## 4.2 Verification of weight convergence and guaranteed control performance

The output from the three layer RBFNN can be written as

$$\hat{v}(k) = [\hat{w}(k)]^{\mathrm{T}}[\psi(z(k))] \tag{52}$$

$\psi(z(k))$, $\hat{w}(k) \in \Re^n$ are the vector of activations of hidden-layer neurons and the vector of current values of connecting weights. Here, the output signal $\hat{v}(k)$ maybe either the NN compensation term of the longitudinal control law (38) or lateral control law (39). The analysis is generalised for both systems and the subscript is omitted for brevity. Expanding (52) into a Taylor series yields

$$v - \hat{v}(k) = [w - \hat{w}(k)]^{\mathrm{T}}[\psi(z(k))] + \zeta \tag{53}$$

where $\zeta$, $|\zeta| < \zeta_N$ represents the neglected higher order terms. With (38), (39), and (53) we obtain

$$\xi'' = \tilde{w}^{\mathrm{T}}\psi(z(k)) + \zeta + \varepsilon \tag{54}$$

where $\tilde{w} = w - \hat{w}(k)$ is the weight estimation error and with $w$, $\|w\| < w_{\max}$ represents the ideal weights. The lateral and longitudinal error dynamics (40), (41) can be written in state-space form as

$$\gamma_x(k+1) = A_x\gamma_x(k) + B_x\xi_1'' \tag{55}$$

$$\gamma_y(k+1) = A_y\gamma_y(k) + B_y\xi_3'' \tag{56}$$

In general

$$\gamma(k+1) = A\gamma(k) + B\xi'' \tag{57}$$

where $\gamma(k) \in \Re^k$ and $(A, B)$ correspond to the state vector and the matrices of the systems (29), (30). Define the error signal to the NN as

$$r(k) = C\gamma(k) \tag{58}$$

For the longitudinal system $C_x = [1\ 1]^{\mathrm{T}}$ and for the lateral system $C_y = [1\ 1\ 1]^{\mathrm{T}}$.

Let the NN weight tuning be provided by

$$\hat{w}(k+1) = \hat{w}(k) + \eta r(k)\psi(z(k)) - \kappa\|\gamma(k)\|\hat{w}(k) \tag{59}$$

$\eta > 0$ is a constant value of adaptation gain and $\kappa > 0$ is a constant design parameter. Jagannathan and Lewis [11, 12] has done extensive analysis on the proof of NN weight convergence for discrete time systems in analytical form. Kumarawadu *et al.* [9] has used the KYP lemma together with the Lyapunov theorem to prove the above in the continuous time domain. In this work we emphasise on the ability to visualise the proof with respect to a difference-Lyapunov surface plot. In order to establish the NN weight convergence under bounded error conditions, we define a Lyapunov function and resort to a graphical technique. Let the candidate Lyapunov function be

$$V(k) = \gamma(k)^{\mathrm{T}}P\gamma(k) + \frac{1}{\eta}\tilde{w}(k)^{\mathrm{T}}\tilde{w}(k) \tag{60}$$

where $P$; $P = P^{\mathrm{T}} \succ 0$ is a solution of the discrete Lyapunov


© The Institution of Engineering and Technology 2010

doi: 10.1049/iet-cta.2009.0144

equation

$$A^{\mathrm{T}}PA - P - Q = 0; \quad Q = Q^{\mathrm{T}} \succ 0 \tag{61}$$

The first difference of the Lyapunov function is

$$\Delta V(k) = V(k+1) - V(k) = \Delta V_1(k) + \Delta V_2(k) \tag{62}$$

where

$$\Delta V_1(k) = \gamma(k+1)^{\mathrm{T}} P \gamma(k+1) - \gamma(k)^{\mathrm{T}} P \gamma(k) \tag{63}$$

$$\Delta V_2(k) = \frac{1}{\eta}\tilde{w}(k+1)^{\mathrm{T}}\tilde{w}(k+1) - \frac{1}{\eta}\tilde{w}(k)^{\mathrm{T}}\tilde{w}(k) \tag{64}$$

With the substitution of (57) into (63) we obtain

$$\Delta V_1(k) = \gamma(k)^{\mathrm{T}}[A^{\mathrm{T}}PA - P]\gamma(k) + 2\gamma(k)^{\mathrm{T}}A^{\mathrm{T}}PB\xi'' + B^{T}PB\xi''^{2} \tag{65}$$

With the substitution of (59) into (64) we obtain

$$\begin{aligned}\Delta V_2(k) = \frac{1}{\eta}[&-\eta\psi^{\mathrm{T}}r^{\mathrm{T}}(k) + \kappa\|\gamma(k)\|\hat{w}(k)^{\mathrm{T}}][w - \hat{w}(k)] \\ &+ [-\tilde{w}(k)^{\mathrm{T}}r(k)\psi + \eta\psi^{\mathrm{T}}r^{\mathrm{T}}(k)r(k)\psi \\ &- 2\kappa\|\gamma(k)\|\hat{w}(k)^{\mathrm{T}}r(k)\psi] \\ &+ \frac{1}{\eta}[\tilde{w}(k)^{\mathrm{T}}\kappa\|\gamma(k)\|\hat{w}(k) \\ &+ \kappa^2\|\gamma(k)\|^2\hat{w}(k)^{\mathrm{T}}\hat{w}(k)]\end{aligned} \tag{66}$$

Considering each term of (65) the following inequalities can be written as

$$\begin{aligned}&-\gamma(k)^{\mathrm{T}}Q\gamma(k) \le -\sigma_{\min}(Q)\|\gamma(k)\|^2 \\ &0 \le \|\psi\| \le \sqrt{n} \\ &\xi'' \le \xi''_{\max}\end{aligned}$$

where

$$\begin{aligned}&\xi''_{\max} = (w_{\max} + \|\hat{w}\|)\sqrt{n} + (\zeta_N + \varepsilon_N) \\ &2\gamma(k)^{\mathrm{T}}A^{\mathrm{T}}PB\xi'' \le 2\|\gamma(k)\|\sigma_{\max}(A^{\mathrm{T}}PB)\xi''_{\max} \\ &B^{\mathrm{T}}PB\xi''^{2} \le \sigma_{\max}(B^{\mathrm{T}}PB)\xi''^{2}_{\max}\end{aligned}$$

Notation $\sigma(\bullet)$ represents the singular value of the vector $(\bullet)$ and the notation $\sigma_{\min}(\bullet)$ represents the minimum singular value of matrix $(\bullet)$.

With the above inequalities we obtain a maximum value function of (63)

$$\begin{aligned}\Delta V_{1,\max} = &-\sigma_{\min}(Q)\|\gamma(k)\|^2 + 2\|\gamma(k)\|\sigma_{\max}(A^{\mathrm{T}}PB)\xi''_{\max} \\ &+ \sigma_{\max}(B^{\mathrm{T}}PB)\xi''^{2}_{\max}\end{aligned} \tag{67}$$

Similarly considering each term of (66) the following inequalities can be written as

$$\begin{aligned}&\hat{w}(k)^{\mathrm{T}}[w - \hat{w}(k)] < \|\hat{w}(k)\|\|w_{\max}\| - \|\hat{w}(k)\|^2 \\ &[2\psi^{\mathrm{T}}r^{\mathrm{T}}(k)][w - \hat{w}(k)] < \sqrt{n}\sigma(C)\|\gamma(k)\|(w_{\max} + \|\hat{w}\|) \\ &\eta\psi^{\mathrm{T}}r^{\mathrm{T}}(k)r(k)\psi \le \eta\|\psi\|^2\|r(k)\|^2 \le \eta n\sigma^2(C)\|\gamma(k)\|^2 \\ &-2\kappa\|\gamma(k)\|\hat{w}(k)^{\mathrm{T}}r(k)\psi \le 2\kappa\sqrt{n}\|\hat{w}(k)\|\sigma(C)\|\gamma(k)\|^2 \\ &\frac{1}{\eta}[\kappa^2\|\gamma(k)\|^2\hat{w}(k)^{\mathrm{T}}\hat{w}(k)] \le \frac{1}{\eta}\kappa^2\|\gamma(k)\|^2\|\hat{w}(k)\|^2\end{aligned}$$

which permit us to write the maximum value function of (64) as

$$\begin{aligned}\Delta V_{2,\max} = &\frac{1}{\eta}[2\kappa\|\gamma(k)\|]\{\|\hat{w}(k)\|\|w_{\max}\| - \|\hat{w}(k)\|^2\} \\ &- \sqrt{n}\sigma(C)\|\gamma(k)\|(w_{\max} + \|\hat{w}\|) \\ &+ \frac{1}{\eta}\kappa^2\|\gamma(k)\|^2\|\hat{w}(k)\|^2 + [\eta n\sigma^2(C)\|\gamma(k)\|^2 \\ &+ 2\kappa\sqrt{n}\|\hat{w}(k)\|\sigma(C)\|\gamma(k)\|^2]\end{aligned} \tag{68}$$

Addition of (67) and (68) yields

$$\Delta V_{\max}(\|\gamma(k)\|, \|\hat{w}(k)\|) = \Delta V_{1,\max} + \Delta V_{2,\max} \tag{69}$$

which satisfies

$$\begin{aligned}&\Delta V(k) \le \Delta V_{\max}(\|\gamma(k)\|, \|\hat{w}(k)\|) \\ &\forall\gamma(k) \in \Re^k, \hat{w}(k) \in \Re^n\end{aligned}$$

Finding a compact set $\mathcal{B} \in \Re^2$ such that

$$\Delta V_{\max}(\|\gamma(k)\|, \|\hat{w}(k)\|) < 0, \quad \forall(\|\gamma(k)\|, \|\hat{w}(k)\|) \notin \mathcal{B}$$

we may guarantee $\Delta V(k) < 0$, $\forall(\|\gamma(k)\|, \|\hat{w}(k)\|) \notin \mathcal{B}$.

Lyapunov theory implies $V(k)$ is bounded and as $k \to \infty$, $(\|\gamma(k)\|, \|\hat{w}(k)\|) \to \mathcal{B}$ manifesting uniform ultimate boundedness (UUB) of dynamics. Thus the weight and error convergence can be certified.

Figs. 4 and 5 show the Lyapunov difference function $\Delta V_{\max}(\|\gamma(k)\|, \|\hat{w}(k)\|)$ surface as well as the contours of the negative transverse of the surface for the longitudinal



© The Institution of Engineering and Technology 2010

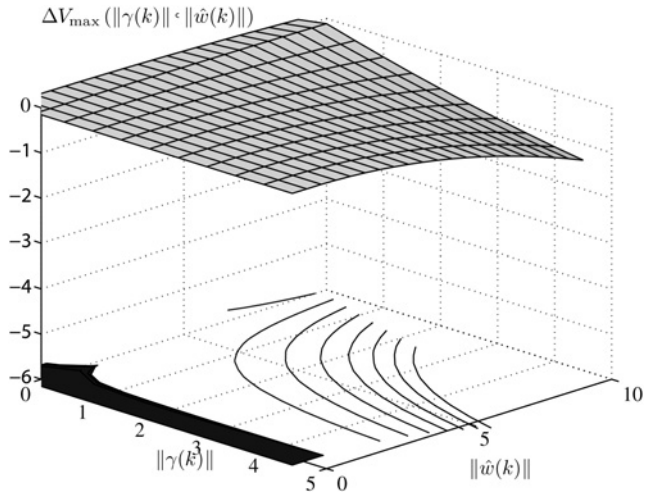


**Figure 4** *Surface and projection of contours in negative transverse of the Lyapunov difference function for the NNs of the longitudinal system*

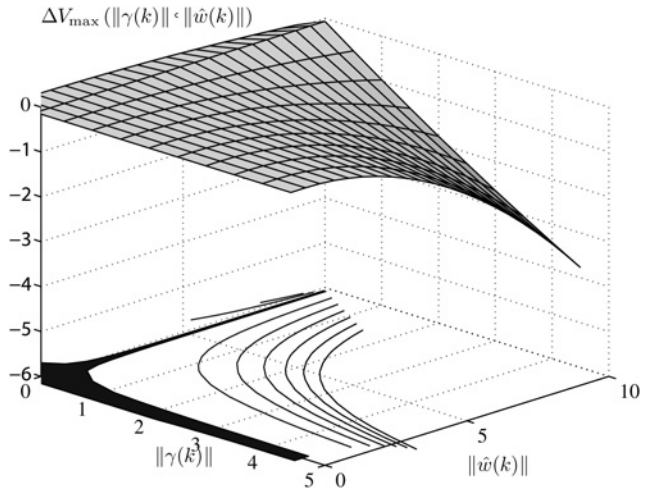


**Figure 5** *Surface and projection of contours in negative transverse of the Lyapunov difference function for the NNs of the lateral system*

and lateral neuro-compensation systems. The surface is obtained for the parameters given in Table 2.

The dark region of the contours represents the compact area in which the surface become briefly positive and can be clearly visualised for both systems. With the NN constraint $\|\hat{w}\| < w_{max}$ and maximum possible $\gamma_{max}$, $\|\gamma(k)\| < \gamma_{max}$ the dark region forms a compact set over the global vector space and therefore error and weight convergence can be guaranteed for both systems. In addition to establishing the weight and error convergence, the surface may also be used in fine tuning the ultimate boundary of $\|\gamma(k)\|$ and $\|\hat{w}(k)\|$.

**Table 2** Parameter values of NNs

| Symbol | Quantity | Value |
|---|---|---|
| $n = n_x = n_y$ | number of hidden neurons | 7 |
| $\eta_x$ | adaptation gain $x$ | 0.01 |
| $\eta_y$ | adaptation gain $y$ | 0.001 |
| $\kappa_x$ | design parameter $x$ | 0.1 |
| $\kappa_y$ | design parameter $y$ | 0.05 |

## 5 Simulation results

Simulations are performed with a controller time step $T_s = 0.005$ s. The continuous time unsimplified vehicle model is simulated with a variable order Adams–Bashforth–Moulton predictor-corrector solver with a maximum time step of 10 μs. The three versions of the control law described earlier are simulated. That is, (i) control law as a linear dynamic state feedback tracking problem with neglected coupling terms and unmodelled dynamics; (ii) control law as a linear dynamic state feedback tracking problem with coupling compensation and neglected unmodelled dynamics; (iii) control law defined as a linear dynamic state feedback tracking problem, with coupling compensation and neuro-compensation of unmodelled dynamics and discretisation approximations. The inputs to the longitudinal NN system is selected as

$$\mathbf{z}_x = \begin{bmatrix} z_1(k) & z_3(k) - z_2(k) & z_1(k-1) & z_4(k) \end{bmatrix}^{\mathrm{T}}$$

and

$$\mathbf{z}_y = \begin{bmatrix} z_1(k) & z_3(k) - z_2(k) & z_2(k) - z_2(k-1) & z_4(k) \end{bmatrix}^{\mathrm{T}}$$

Longitudinal spacing $\Delta_x$ and lateral deviation $z_3^*(k)$ are selected as 10 and 0 m. The preceding vehicle velocity, the road profile used for this simulation and the road curvature is given in Fig. 6. The road curvature is selected with high values such as 0.16 $\mathrm{m}^{-1}$ and preceding vehicle speed is selected with high

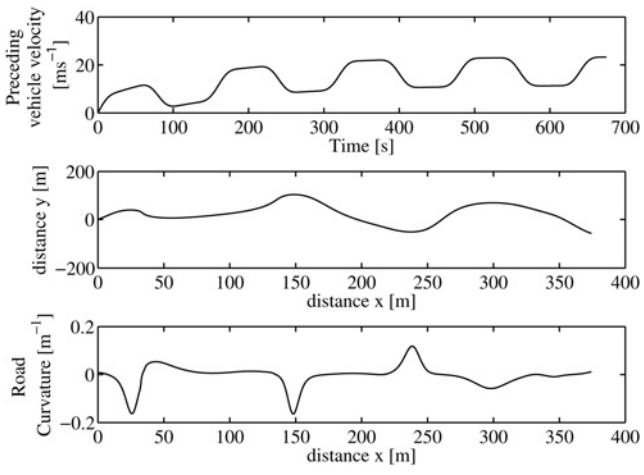


**Figure 6** *Road and velocity characteristics*


© The Institution of Engineering and Technology 2010

doi: 10.1049/iet-cta.2009.0144

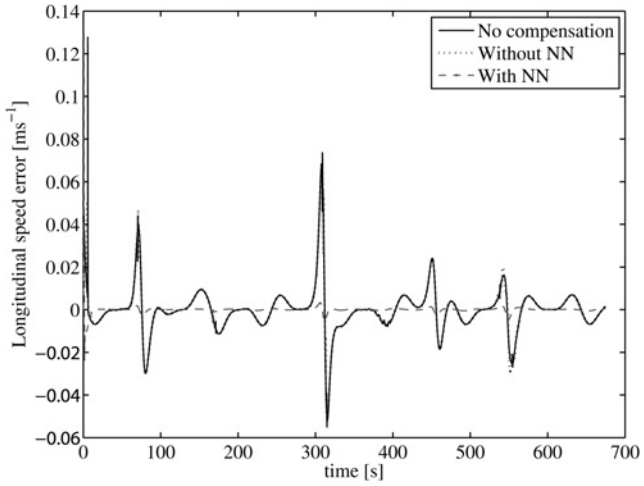


**Figure 7** *Longitudinal speed error*

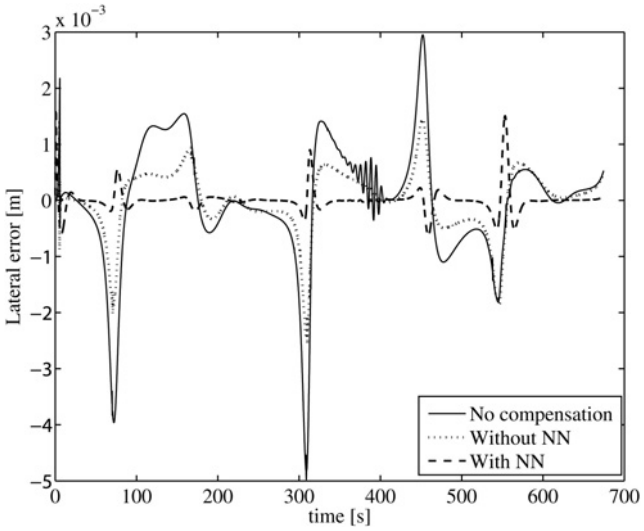


**Figure 8** *Lateral spacing error*

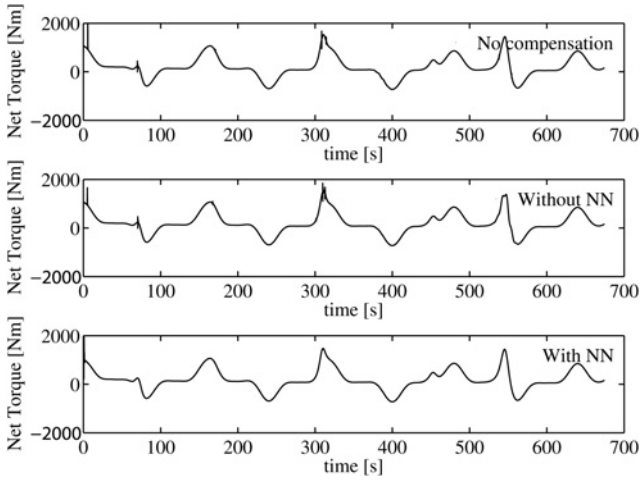


**Figure 9** *Net torque*

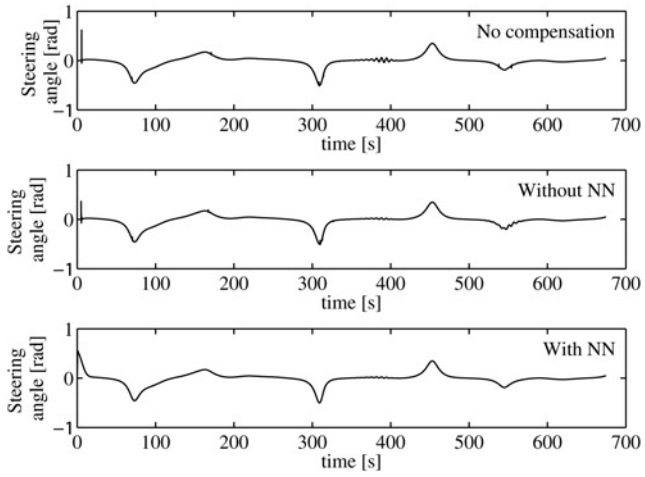


**Figure 10** *Steering angle*

accelerations to represent worst-case situations where the vehicle may have to negotiate sharp turns at high speed.

Figs. 7 and 8 present the longitudinal and lateral spacing error for parameters differing from the ideal values considering a worst-case variation of each. That is, with $m = \hat{m} + 300$, $I_Z = (m/\hat{m})\hat{I}_Z$, $C_f = 0.75\hat{C}_f$, $C_r = 0.75\hat{C}_r$, $k_L = 1.1\hat{k}_L$ and $k_D = 1.1\hat{k}_D$. The practical bounds for acceleration capability of the vehicle is assumed to be given by $110250.0/mz_1(k)$ for $z_1(k) \geq 12.5$ ms$^{-1}$ and 3 ms$^{-2}$ otherwise.

Figs. 9 and 10 presents the net torque demand from the engine and the steering angle of the vehicle for the three cases considered.

## 6 Conclusions

Three versions of the discrete-time controller development are compared. Based on the simulation results, the dynamic state feedback control mechanism alone is found to offer adequate performance under limited speed and road curvature conditions. The first phase of the controller stabilises the longitudinal and lateral systems locally with dynamic state feedback architecture and is tuned with linear quadratic optimisation for good gain margin and phase margin. The neglected non-linearities are estimated and compensated in the second phase. Additional neglected dynamics and approximations are compensated with a neuro-adaptation term in the third phase. The NN weights are initialised at zero and are adapted online without and off-line training. The weight and error convergence in UUB is established via a graphical technique based on Lyapunov theory.

Even though the non-linear coupling compensation in both the lateral and longitudinal systems is of the same order in magnitude, the relative magnitude of state variables of the lateral speed and yaw-rate are small compared with the longitudinal speed. Hence, under typical and slightly severe manoeuvres for highway vehicles, the visible effect of non-linear coupling compensation on



© The Institution of Engineering and Technology 2010

lateral dynamics is much higher than that of the longitudinal dynamics. However, non-linear coupling compensation on longitudinal dynamics can be much more important when the vehicle is negotiating emergency situations or performing lane-changing manoeuvers where larger steering inputs are needed.

It can be inferred from the results that the unmodelled dynamics significantly affect the acceleration of the vehicle especially at high speeds and large road curvatures. Uncertainties in the vehicle mass directly affect the controller performance. In both cases without any NN compensation, higher vehicle mass than the estimated value will damp the speed response of the vehicle. Neuro-compensation takes into account the error in mass estimation and improves the vehicle speed response significantly. In comparison, the NN unmodelled dynamics compensation has a higher effect on the overall performance of the vehicle compared with the inclusion of the non-linear coupling compensation. Control without unmodelled dynamics compensation will require the vehicle to operate with a higher safety margin. In contrast, the addition of neuro-compensation will enable the vehicle to operate with lower margins on speed, relative distance giving an extended IVHS safe operating speed-curvature regime.

Future work will involve analysis of the controller performance with different sensory systems in addition to the existing magnetic marker and radar-based measurements. The advantage of extended speed-curvature range for the presented controller will be established and compared with other existing controllers. The processing power requirements and limitations of industrial microprocessor-based implementation and sampling time requirements will be further analysed.

# 7 References


[1] MAR J., LIN F.J.: 'An ANFIS controller for the car-following collision prevention system', *IEEE Trans. Veh. Technol.*, 2001, **50**, (4), pp. 1106–1113

[2] HINGWE P.: 'Robustness and performance issues in the lateral control of vehicles in automated highway systems'. PhD dissertation, University California, Berkeley, CA, 1997

[3] NARANJO J.E., GONZLEZ C., REVIEJO J., GARCA R., DE PEDRO T.: 'Adaptive fuzzy control for inter-vehicle gap keeping', *IEEE Trans. Intell. Transp. Syst.*, 2003, **4**, (3), pp. 132–142

[4] CAI L., RAD A.B., CAI K.Y.: 'A robust fuzzy PD controller for automatic steering control of autonomous vehicles'. Proc. IEEE Int. Conf. on Fuzzy Syst., St. Louis, MO, 2003, pp. 549–554

[5] KALKKUHL J., HUNT K.J., FRITZ H.: 'FEM-based neural network approach to nonlinear modeling with application to longitudinal vehicle dynamics control', *IEEE Trans. Neural Netw.*, 1999, **10**, (4), pp. 885–897

[6] LIM E.H.M., HEDRICK J.K.: 'Lateral and longitudinal vehicle control coupling for automated vehicle operation'. Proc. American Control Conf., 1999, pp. 3676–3680

[7] CHOI S., HEDRICK J.K.: 'Vehicle longitudinal control using an adaptive observer for automated highway systems'. Proc. American Control Conf., 1995, vol. 5, pp. 3106–3110

[8] NOBE S.A., WANG F.Y.: 'An overview of recent developments in automated lateral and longitudinal vehicle controls'. Proc. IEEE Int. Conf. on Syst. Man, and Cybern., Tucson, AZ, 2001, vol. 5, pp. 3447–3452

[9] KUMARAWADU S., LEE T.T.: 'Neuroadaptive combined lateral and longitudinal control of highway vehicles using RBF networks', *IEEE Intell. Transp. Syst.*, 2006, **7**, (4), pp. 500–512

[10] ZHANG M., NAGAMATSU A.: 'Motion control of flexible arm by using neuro-adaptive control: LQN control system and numerical simulation'. Proc. IEEE 25th Ann. Conf., IECON'99, 1999, vol. 2, pp. 990–995

[11] JAGANNATHAN S., LEWIS F.L.: 'Discrete-time neural net controller with guaranteed performance'. Proc. American Control Conf., June 1994

[12] JAGANNATHAN S., LEWIS F.L.: 'Discrete-time neural net controller for a class of nonlinear dynamical systems', *IEEE Trans. Autom. Control.*, 1996, **41**, (11), pp. 1693–1699

[13] REN X.M., RAD A.B., CHAN P.T., WAI LUN LO: 'Identification and control of continuous-time nonlinear systems via dynamic neural networks', *IEEE Trans. Ind. Electron.*, 2003, **50**, (3), pp. 478–486

[14] KANELLAKOPOULOS I., KOKOTOVIC P.V., MARINO R.: 'An extended direct scheme for robust adaptive nonlinear control', *Automatica*, 1991, **27**, pp. 247–255

[15] NOURI K., DHAOUADI R., BENHADJ BRAIEK N.: 'Adaptive control of a nonlinear dc motor drive using recurrent neural networks', *Appl. Soft Comput.*, 2008, **8**, (1), pp. 371–382

[16] PLETT G.L.: 'Adaptive inverse control of linear and nonlinear systems using dynamic neural networks', *IEEE Trans. Neural Netw.*, 2003, **14**, (2), pp. 360–376

[17] LU G.: 'Robust observer design for lipschitz nonlinear discrete-time systems with time-delay'. Ninth Int. Conf. on Control, Automation, Robotics and Vision, ICARCV'06, 5–8 December 2006, pp. 1–5

[18] HERNANDEZ J.I., KUO C.Y.: 'Steering control of automated vehicle using absolute positioning GPS and magnetic markers', *IEEE Trans. Veh. Technol.*, 2003, **52**, (1), pp. 150–161



© The Institution of Engineering and Technology 2010

doi: 10.1049/iet-cta.2009.0144

[19] LEE H., TOMIZUKA M.: 'Coordinated longitudinal and lateral motion control of vehicles for IVHS', *Trans. ASME J., Dyn. Syst. Meas. Control*, 2001, **123**, (3), pp. 535–543

[20] ROSENBLUM M., DAVIS L.S.: 'An improved radial basis function network for autonomous road following', *IEEE Trans. Neural Netw.*, 1996, **7**, (5), pp. 1111–1120

[21] MCMAHON D.H., NARENDRAN V.K., HEDRICK J.K.: 'Longitudinal vehicle controllers for IVHS: theory and experiments'. Proc. American Control Conf., 1992, pp. 1753–1757

[22] BARTOLINI G., FERRARA A., PISU P.: 'Longitudinal control design of passenger vehicles with second order sliding modes'. Proc. American Control Conf., 2000, vol. 1, no. 6, pp. 120–124

[23] PHAM H.: 'Combined lateral and longitudinal control of vehicles for the automated highway systems'. PhD dissertation, University California, Berkeley, CA, 1996

[24] TAM T., BEJCZY A., YUN X.: 'Robot arm force control through system linearization by nonlinear feedback'. IEEE Conf. on Robotics and Automation, 1988, pp. 1618–1625

[25] PHAM H., HEDRICK J.K., TOMIZUKA M.: 'Combined lateral and longitudinal control of vehicles for IVHS'. Proc. American Control Conf., 1994, pp. 1205–1206

[26] ANDERSON B.D.O., MOORE J.B.: 'Optimal control: linear quadratic methods' (Prentice-Hall, Englewood Cliffs, NJ, 1989)

[27] ZHANG C., FU M.: 'A revisit to the gain and phase margins of linear quadratic regulators', *IEEE Trans. Autom. Control*, 1996, **14**, (10), pp. 1527–1530

[28] FUNAHASHI K.: 'On the approximate realization of continuous mappings by neural networks', *Neural Netw.*, 1989, **2**, pp. 183–192

[29] CYBENKO G.: 'Approximation by superposition of a sigmoidal function'. Technical report, Department of Electronics and Computer Enginerring, University Illinois at Urbana-Champaign, 1988

[30] HORNIK K., STINCHCOMBE M., WHITE H.: 'Multilayer feedforward networks are universal approximators', *Neural Netw.*, 1989, **2**, pp. 359–366

[31] HAYKIN S.: 'Neural networks: a comprehensive foundation' (Prentice-Hall, Englewood Cliffs, NJ, 1999, 2nd edn.)

[32] KHAN M.I., FRAYMAN Y., NAHAVANDI S.: 'Mixed transfer function neural networks for knowledge acquisition'. IEEE Int. Conf. on Industrial Technology, ICIT 2009, 10–13 February 2009, pp. 1–6

[33] LEWIS F.L.: 'Neural network control of robot manipulators', *IEEE Expert*, 1996, **11**, (3), pp. 64–75

[34] CHEN S., COWAN C., GRANT P.: 'Orthogonal least squares learning algorithm for radial basis function networks', *IEEE Trans. Neural Netw.*, 1991, **2**, (2), pp. 302–309

[35] Progress in Supervised Neural Networks: 'What's new since Lippmann'. IEEE Signal Process. Magazine, 1993, pp. 8–39

[36] MOODY J., DARKEN C.: 'Fast learning in networks of locally-tuned processing units', *Neural Comput.*, 1989, **1**, (2), pp. 281–294

[37] PARK J., SANDBERG I.W.: 'Universal approximation using radial-basis-function networks', *Neural Comput.*, 1991, **3**, (2), pp. 246–257

[38] PAPAIOANNOU I.V., ROUSSAKI I.G., ANAGNOSTOU M.E.: 'Comparing the performance of MLP and RBF neural networks employed by negotiating intelligent agents'. IEEE/WIC/ACM Int. Conf. on Intelligent Agent Technology, IAT'06, 18–22 December 2006, pp. 602–612



© The Institution of Engineering and Technology 2010